Published in final edited form as:

Eur J Cell Biol. 2023 September ; 102(3): 151339. doi:10.1016/j.ejcb.2023.151339.

Receptor-mediated internalization promotes increased endosome size and number in a RAB4- and RAB5-dependent manner

Naava Naslavsky[a,b], **Steve Caplan**[a,b,*,1]

[a]Department of Biochemistry & Molecular Biology, University of Nebraska Medical Center, Omaha, NE 68198, USA

[b]Fred and Pamela Buffett Cancer Center, University of Nebraska Medical Center, Omaha, NE 68198, USA

Abstract

Despite their significance in receptor-mediated internalization and continued signal transduction in cells, early/sorting endosomes (EE/SE) remain incompletely characterized, with many outstanding questions that surround the dynamics of their size and number. While several studies have reported increases in EE/SE size and number resulting from endocytic events, few studies have addressed such dynamics in a methodological and quantitative manner. Herein we apply quantitative fluorescence microscopy to measure the size and number of EE/SE upon internalization of two different ligands: transferrin and epidermal growth factor. Additionally, we used siRNA knock-down to determine the involvement of 5 different endosomal RAB proteins (RAB4, RAB5, RAB8A, RAB10 and RAB11A) in EE/SE dynamics. Our study provides new information on the dynamics of endosomes during endocytosis, an important reference for researchers studying receptor-mediated internalization and endocytic events.

Keywords

Internalization; Endosome size; Endosome number; RAB4; RAB5; RAB8A; RAB10; RAB11A

[1]ORCID297

[*]Corresponding author at: Department of Biochemistry & Molecular Biology, University of Nebraska Medical Center, Omaha, NE 68198, USA. scaplan@unmc.edu (S. Caplan).

CRediT authorship contribution statement

Naava Naslavsky: Conceptualization, Validation, Formal analysis, Investigation, Writing – review & editing, Visualization. **Steve Caplan:** Conceptualization, Formal analysis, Writing – original draft preparation, Supervision, Project administration, Funding acquisition.

Declaration of Competing Interest

The authors declare that they have no known competing financial interests or personal relationships that could have appeared to influence the work reported in this paper.

Appendix A. Supporting information

Supplementary data associated with this article can be found in the online version at doi:10.1016/j.ejcb.2023.151339.

1. Introduction

The process of receptor-mediated endocytosis, also known as receptor uptake or receptor internalization, is essential for all eukaryotic cells (Conner and Schmid, 2003). Once internalized, either by clathrin-dependent or independent endocytosis, the newly-internalized vesicles fuse and deliver their receptor cargo to a membrane-bound internal compartment known as the early or sorting endosome (EE/SE) (Jovic et al., 2010). EE/SE are defined as having a limiting bilayer membrane enriched in the phosphoinositide phosphatidyl 3-phosphate (PI3P) that binds to select FYVE domain-containing proteins such as EEA1 (Corvera et al., 1999; Kobayashi et al., 1998), and an acidic lumenal pH of ~6.2 that is sufficient to separate most ligands from their receptors (Murphy et al., 1984). Crucial receptor sorting events occur in EE/SE, dictating whether they are recycled to the plasma membrane or transported to the lysosomal pathway for degradation, thus controlling the cell's response to external stimulation (Naslavsky and Caplan, 2018). Moreover, recent studies suggest that receptors continue to signal from endosomes (Miaczynska and Bar-Sagi, 2010).

Despite their significance, many basic questions remain unanswered regarding the generation of endosomes, the process of their maturation and/or relationship to one another, and their function as organelles that sort cargo for transport and facilitate continued signal transduction once receptors have been transported to endosomes (Naslavsky and Caplan, 2018). In particular, EE/SE remain incompletely characterized. For example, several studies have indicated that inducing receptor mediated internalization in cells leads to increased numbers of EE/SE and an increase in their size (Benveniste et al., 1989; Nossal et al., 1983; Parton et al., 1992; Robert et al., 1985). In addition, endosome size is regulated by RAB4 and RAB5 (Duclos et al., 2003; Haas et al., 2005; Tubbesing et al., 2020; Zeigerer et al., 2012) as well as other factors (Dilsizoglu Senol et al., 2019; Ramanathan and Ye, 2012). As noted above, endosome size and number are crucially important parameters because signaling is thought to continue in endosomes following receptor internalization from the plasma membrane (Villasenor et al., 2015). In addition, effective drug targeting requires endosomal escape of internalized drugs to the cytoplasm and studies have demonstrated that endosome size influences likelihood of endosome escape (Vermeulen et al., 2018). Although a multitude of studies has addressed exosome size (Raposo and Stoorvogel, 2013), and additional studies have focused on lysosome size (de Araujo et al., 2020), over the past four decades relatively few studies have addressed how endosome size and number are impacted by internalization events and by key Rab proteins.

Herein, we use quantitative microscopy to measure key EE/SE parameters in non-small cell lung cancer cells and HeLa cells, including EE/SE number and area under steady-state conditions as well as conditions where receptor mediated internalization was induced by incubating cells with two different ligands: either transferrin (Tf) or epidermal growth factor (EGF). In addition, we undertook an siRNA knockdown strategy for 5 different RAB proteins, including RAB4, RAB5, RAB8A, RAB10 and RAB11A, to assess the impact on EE/SE number and size for both steady state and subsequent to receptor-mediated endocytosis. Overall, this study provides a concise but much-needed atlas for EE/SE that

will serve as an important reference for researchers who study internalization and endocytic events.

2. Results

2.1. Receptor-mediated endocytosis leads to increased size and number of EE/SE

To address how the size and number of EE/SE is affected by internalization, we incubated non-small cell lung cancer (NSCLC) cells for 15 min in the presence or absence of transferrin (Tf) to induce clathrin-mediated internalization of the transferrin receptor (TfR) (Pearse, 1982), and then quantified the mean area and number of EEA1-marked EE/SE, as EEA1 is one of the best-characterized endosomal markers (Mu et al., 1995). We have previously used these NSCLC cells as a model for studying trafficking, because they are large, homogeneous, and easy to visualize microscopically (Cai et al., 2014). As demonstrated, the mean area of EE/SE increased from a baseline of 1.83 μm^2 in cells that were not subjected to Tf uptake to 3.17 μm^2 upon Tf uptake, reflecting a statistically significant 58% increase (Fig. 1A; see C and D for representative images illustrating “no uptake” and “Tf uptake,” respectively). Moreover, the mean number of EEA1-marked EE/SE per field of cells with no Tf uptake was 2223, whereas uptake with Tf increased the number of EE/SE to 4148, representing a statistically significant 54% increase, similar to the increase observed in EE/SE mean area (Fig. 1B; see C and D for representative images). Indeed, in NSCLC cells, we found that whereas about 56% of EEA1-containing endosomes overlapped with RAB5-containing endosomes, only ~45% of RAB5-containing endosomes overlapped with EEA1-containing endosomes, highlighting that RAB5 marks a larger population of endosomes than EEA1 (Supplemental Fig. 1). In HeLa cells, this difference was even more dramatic, with about 75% of EEA1-containing endosomes overlapping with RAB5-containing endosomes, and only ~56% of RAB5-containing endosomes overlapping with EEA1-containing endosomes (Supplemental Fig. 1). Overall, these data clearly indicate that receptor mediated internalization of TfR leads to a rapid 50–60% increase in the size and number of EE/SE in NSCLC cells.

TfR is unusual in that it binds to its ligand, iron-laden holo-transferrin, and does not dissociate in endosomes but is instead recycled with the receptor back to the plasma membrane after the iron bound to the Tf is released (Apo-transferrin) in the acidic environment of the endosome (Ciechanover et al., 1983). Accordingly, we asked whether internalization of another clathrin-mediated receptor (Sorkin et al., 1996), epidermal growth factor receptor (EGFR), similarly impacts EE/SE size and number, and incubated non-small cell lung cancer cells for 15 min with epidermal growth factor (EGF). In these experiments using a different ligand/receptor pair, we also elected to vary our endosomal marker and used RAB5, which has been studied as an endosomal protein and regulator for over 30 years (Bucci et al., 1992; Gorvel et al., 1991). As demonstrated, the mean area of RAB5-marked EE/SE in the absence of EGF was 1.68 μm^2 (Fig. 2A; see C and D for representative images), in a similar range to the mean area for EE/SE of the untreated cells immunostained with EEA1 in Fig. 1A. Upon incubation with EGF, the mean area of the RAB5-marked EE/SE increased by 56% to 3.02 μm^2 (Fig. 2A; see C and D for representative images), consistent with the data obtained for EEA1-marked EE/SE size upon Tf uptake in Fig.

1A. The number of “baseline” RAB5-marked EE/SE in untreated cells at steady-state was 5480 (Fig. 2B). Upon EGF uptake, RAB5-marked EE/SE increased by 58% to 9483, again consistent with the percent increase in EEA1-marked EE/SE observed upon incubation with Tf (Fig. 1B). Overall, these data indicate that clathrin-mediated endocytosis of different receptors stimulates a similar increase in size and number of either EEA1- or RAB5-marked EE/SE, potentially allowing the cell to handle enhanced amounts of incoming internalized lipids and receptors from the plasma membrane.

RAB proteins are key regulators of endocytic trafficking, and both RAB4 and RAB5 localize to EE/SE and have been implicated in endosome biogenesis (Barbieri et al., 1996; Bucci et al., 1992; Gorvel et al., 1991; van der Sluijs et al., 1992; Van Der Sluijs et al., 1991). While RAB8, RAB10 and RAB11 are also considered endosomal RAB proteins (Babbey et al., 2006; Chen et al., 1993; Green et al., 1997; Huber et al., 1993; Linder et al., 2007; Ullrich et al., 1996), evidence suggests that they act at later recycling endosomal compartments and their potential impact on EE/SE is not as well characterized. Accordingly, we aimed to determine how these well-characterized endosomal RAB proteins influence endosome size and number, both in steady-state and in cells subjected to receptor-mediated internalization. To address this question, we first used siRNA knock-down in HeLa cells to deplete RAB4, RAB5, RAB8A (which is the major RAB8 expressed in HeLa cells), RAB10 and RAB11A (the major RAB11 expressed in HeLa cells). In these experiments, the HeLa cells were used because they serve as a well-characterized model for membrane trafficking and the cells are readily amenable to siRNA knock-down (Naslavsky et al., 2006; Rahajeng et al., 2012; Zhang et al., 2012). As demonstrated, whereas vinculin levels remained relatively constant in mock-treated and siRNA-knock-down cells, each of the 5 RAB proteins could be readily depleted upon siRNA treatment (Fig. 3A). Mock-treated and RAB knock-down cells were then incubated for 15 min in the presence or absence of Tf, fixed, imaged and subjected to quantification to determine the mean number of EEA1-marked EE/SE per field of cells (Fig. 3H; representative images of fields of cells without Tf uptake are depicted in Fig. 3B–G), and the mean area of EEA1-marked sorting endosomes (Fig. 3I). As demonstrated earlier, mock-treated cells subjected to transferrin uptake displayed a statistically significant increase in EEA1-marked EE/SE number and area compared to naïve cells, albeit less pronounced than that observed in the non-small cell lung cancer cells (Fig. 3H and I). Both RAB4-depletion and RAB5-depletion led to significantly decreased numbers and area of EE/SE at steady-state compared to mock-treated cells, highlighting the requirement of these two RAB proteins in EE/SE biogenesis and/or maintenance. However, the addition of Tf to cells depleted of either RAB4 or RAB5 did lead to robust increases in EE/SE numbers and area, although they did not reach the baseline levels observed in mock-treated cells. These data suggest that while the ability to generate new EE/SE is maintained in RAB4 and RAB5 knock-down cells, the primary deficit observed is the decreased number and area of EE/SE observed at steady-state. Despite their role in endocytic membrane trafficking, steady-state numbers and area of EE/SE in RAB8A, RAB10 and RAB11A knock-down cells remained similar to those observed in the mock-treated cells. However, unlike the mock-treated cells, RAB4 knock-down and RAB5 knock-down cells, Tf uptake in RAB8A- and RAB10-depleted cells did not induce increased numbers and area of EE/SE, and in RAB11A depleted cells, the number and area of EE/SE even decreased significantly

compared to naïve cells not incubated with Tf. Interestingly, while the area of EEA1 endosomes displayed a significant decrease in RAB10 knock-down cells incubated with transferrin, only a slight a non-significant decrease in endosome number was noted. Overall these findings demonstrate the selective roles of RAB proteins at EE/SE, emphasizing essential roles for RAB4 and RAB5 in control of EE/SE number, suggesting other important functions for RAB8A, RAB10 and RAB11 “downstream” at more specialized endosomes, such as recycling endosomes.

3. Discussion

Endocytic membrane trafficking is essential for crucial cellular functions, and specifically for control of receptor-mediated signal transduction ultimately leading to cell migration, differentiation and proliferation. As such, a comprehensive understanding of the endosome, including characterization of size and number under steady-state conditions and upon receptor-mediated internalization, is well-warranted. Despite the urgency for such information, and although technology for imaging quantification has improved dramatically within the last decade, only a handful of studies directly address these points (Benveniste et al., 1989; Nossal et al., 1983; Parton et al., 1992; Robert et al., 1985), and it remains difficult to obtain basic information about the size and number of endosomes in the cell, and how they are influenced by internalization events. However, despite the use of advanced imaging and quantification software that allows for powerful analysis, we are aware of potential shortcomings in our methodologies. These include heavy reliance on the specificity of siRNA oligonucleotides used in the study and the antibodies used for marking endosomes. Fortunately, these antibodies and siRNAs are well characterized and have well-documented selectivity, and the ability to study endogenous proteins in this study increases its relevance.

In the current study, we demonstrate significant 50–60% increases in the number and size of endocytic structures designated as early/sorting endosomes in non-small cell lung cancer cells, upon receptor-mediated internalization of either TfR or EGFR. This increase in total EE/SE volume within the cell highlights the capacity for cellular adaptivity upon conditions of marked internalization. However, it also demonstrates the need for efficient recycling of lipids back to the plasma membrane after internalization, allowing the cell to maintain the surface area of its limiting membrane and preventing shrinkage.

While the size of the EEA1-marked endosomes (with or without Tf uptake) was consistent with that of RAB5-marked endosomes (with or without EGF uptake), it is notable that overall numbers of RAB5-marked endosomes, both at baseline and following internalization, ranged about 2-fold higher than EEA1-marked endosomes. The most likely explanation for this difference is that EEA1-marked endosomes represent only a subset of RAB5-marked endosomes, although we cannot rule out the possibility of differences in the affinities and/or selectivity of the antibodies to these two proteins. As we demonstrate in Supplemental Fig. 1, significantly more EEA1 overlaps with RAB5 than RAB5 overlaps with EEA1, supporting the idea that RAB5 endosomes represent a broader proportion of EE/SE. Nonetheless, the similar proportion of increase in size and number of endosomes observed upon uptake of either Tf or EGF suggests that the EEA1 and RAB5 endosomal

populations are at least partially overlapping, consistent with their interaction (Christoforidis et al., 1999a; Simonsen et al., 1998).

While serving as a useful marker for EE/SE, RAB5 is also an essential protein involved in EE/SE biogenesis, maturation, and fusion (Christoforidis et al., 1999a; Christoforidis et al., 1999b; Schnatwinkel et al., 2004; Simonsen et al., 1998; Vitale et al., 1998). RAB4 has also been identified as a key EE/SE protein (Daro et al., 1996; de Wit et al., 2001; van der Sluijs et al., 1992; Van Der Sluijs et al., 1991). However, dozens of additional RAB proteins play a wide variety of roles in the control of endocytic transport (Pfeffer, 2017). Accordingly, we chose to study 3 additional RAB proteins that have been implicated in trafficking at recycling endosomes, typically considered downstream from EE/SE: RAB8A, RAB10 and RAB11A. RAB8A binds to the EHD1 binding partner MICAL-L1 (Rahajeng et al., 2012; Sharma et al., 2010; Sharma et al., 2009), and has been implicated in a variety of endocytic membrane trafficking events, including the regulation of primary ciliogenesis (Ang et al., 2003; Feng et al., 2012; Huber et al., 1993; Knodler et al., 2010; Linder et al., 2006; Sato et al., 2007). Rab10 has also been implicated in the regulation of ciliogenesis and trafficking in multiple pathways, and in the generation of tubular recycling endosomes (Babbey et al., 2006; Babbey et al., 2010; Chen and Lippincott-Schwartz, 2013; Chen et al., 1993; English and Voeltz, 2013; Etoh and Fukuda, 2019; Farmer et al., 2020; Schuck et al., 2007). RAB11A is also involved in primary ciliogenesis and has been well-documented as a key RAB on recycling endosomes (Green et al., 1997; Kobayashi and Fukuda, 2013; Ullrich et al., 1996). Our data are consistent with the notion that RAB4 and RAB5 are central EE/SE regulators, and we have demonstrated that depletion of either protein leads to a major decrease in the number and size of EEA1-marked EE/SE at steady-state (Fig. 3H and I; representative data shown in 3B-G). Indeed, RAB5 depletion at steady-state showed a ~4-fold decrease in the number of EE/SE and a similar decrease in EE/SE size compared to mock-treated cells, consistent with its essential role in the fusion of incoming uncoated vesicles with EE/SE (Gorvel et al., 1991). RAB4 depletion led to a ~2-fold decrease in the number of EE/SE per field of cells and a ~3-fold decrease in EE/SE size, also consistent with its role in EE/SE regulation (van der Sluijs et al., 1992; Van Der Sluijs et al., 1991). In contrast to RAB4 and RAB5, little difference was observed in steady-state numbers of EE/SE or endosome size in cells depleted of RAB8A, RAB10 or RAB11A, strongly suggesting that these RAB proteins are indeed downstream of RAB4 and RAB5. Somewhat intriguingly, despite RAB5 depletion having such a dramatic effect on the steady-state levels of EE/SE and their size, the induction on Tf internalization in these cells stimulated a dramatic increase in EE/SE generation and a parallel increase in endosome size. Given that RAB4 depleted cells also show an increase in EE/SE upon Tf uptake (albeit less dramatic), we speculate that RAB4 and RAB5 may partially compensate for one another (potentially along with additional RAB proteins), thus facilitating increased endosome volume upon internalization. While it would be optimal to test this notion by double knock-down of RAB4 and RAB5, our inability to achieve simultaneous efficient reduction of both RABs renders it difficult to make valid interpretations. Future studies may benefit from CRISPR knockouts of both RABs, which ultimately may be required to address the potential role of compensation between RAB4 and RAB5. Rab11A siRNA knock-down efficiency was relatively modest compared to knock-downs of the other RAB

proteins in this study. However, of the RAB proteins depleted, we observed that RAB11A depletion had a surprising cellular phenotype; there was little effect on EE/SE numbers at steady-state compared to mock-treated cells, but upon internalization, EE/SE numbers decreased significantly. While it is difficult to explain this phenomenon, one possibility is that RAB11 prevents exit from EE/SE, leading to a buildup in endosomes. However, this notion is not supported by the concomitant decrease in EE/SE size (as well as number) upon RAB11 knock-down. It is possible to speculate that as a major RAB protein required for recycling pathways, increased retention of receptors within the cell might lead to decreased internalization at the plasma membrane, and thus indirectly lead to reduced numbers of EE/SE. Indeed, a number of studies support the notion of increased levels of cell surface receptors upon knock-down of RAB4 (Binda et al., 2019), RAB5 (Kageyama-Yahara et al., 2011; Yang et al., 2015) and RAB11 (Keil and Hatzfeld, 2014).

We are cognizant that in selecting RAB4, RAB5, RAB8A, RAB10 and RAB11A for this study, the roles of many other key small GTP-binding proteins within the endocytic pathways are not addressed. Particularly relevant are RAB21 (Simpson et al., 2004), RAB22A (Magadan et al., 2006), RAB35 (Kouranti et al., 2006; Rahajeng et al., 2012), RAB13 (Terai et al., 2006), RAB14 (Jagath et al., 2004), RAB15 (Zuk and Elferink, 1999), RAB36 (Kobayashi et al., 2014) and ARF6 (Brown et al., 2001; Naslavsky et al., 2003), although other RABs are likely also involved at the endosomes.

Overall, this study provides key basic information regarding the number and size of endosomes in steady-state and upon internalization of different receptors. Coupled with new information comparing key endosomal RAB proteins in the regulation of EE/SE number and size in cells, we anticipate that our observations will be beneficial to the many researchers interested in endosomes, with implications for those studying drug targeting into cells and endosomal escape.

4. Materials and methods

4.1. Antibodies and reagents

Primary and secondary antibodies used in this study were rabbit anti-EEA1 (Cell Signaling cat. no. C45810), mouse anti-RAB5 (BD Transduction Labs cat. no. 610724), mouse anti-RAB4 (BD Transduction Labs cat. no. 610889), rabbit anti-RAB8 (Abcam cat no. 237702), rabbit anti-RAB10 (Abcam cat. no. 237703), mouse anti-RAB11 (BD Transduction Labs cat. no. 610657), HRP-conjugated anti-vinculin (Cell Signaling cat no. E1E9V XP), goat anti-mouse horseradish peroxidase (HRP), (cat. no. 115–035–003; Jackson ImmunoResearch Laboratories, West Grove, PA), donkey anti-rabbit HRP (cat. no. NA934V; GE Healthcare, Pittsburgh, PA), Alexa 568–conjugated goat anti-mouse (cat. no. A11031), and Alexa 488–conjugated goat anti-rabbit (cat. no. A11034; Life Technologies, Carlsbad, CA). Transferrin labeled with Alexa-568 (Tf-568; Molecular Probes cat. no. T23365) and epidermal growth factor labeled with Alexa-555 (EGF-555; Molecular Probes cat. no. E35350) were obtained from ThermoFisher Scientific.

siRNA	Company	Cat. no.	Sequence	Concentration (nmol)
Rab4	Dharmacon	custom	AACCUACAAUCGGCUUACUAA	280
Rab5	Sigma	97508	GUCCUAUGCAGAUGACAAU	400
Rab8A	Sigma	339466	GAGACCAGCGCGAAGGCCA	600
Rab10	Dharmacon	L-010823	On-Target	400
Rab11A	Sigma	126206	CAGAACAUCUAAGGCAUUU	600

4.2. Cell culture and treatments

Hela cells from ATCC (ATCC cat. no. CCL-2) were grown at 37 °C in 5% CO_2 in DMEM (Thermo Fisher Scientific) containing 10% fetal bovine serum (FBS; Sigma-Aldrich), 2 mM L-glutamine, 100 U/ml penicillin/streptomycin (ThermoFisher Scientific). Non-small cell lung cancer cells from ATCC (NCI-H1650; ATCC cat. no. CRL-5883) were grown at 37 °C in 5% CO_2 in RPMI (Thermo Fisher Scientific) containing 10% fetal bovine serum (FBS; Sigma-Aldrich), 2 mM L-glutamine, 100 U/ml penicillin/streptomycin and 1X non-essential amino acids (ThermoFisher Scientific). All cell lines in the laboratory are also grown in 100 mg/ml Normocin (ThermoFisher Scientific) to prevent mycoplasma and other contamination and routinely tested for mycoplasma contamination. SiRNA knockdown of RAB protein expression in HeLa cells was carried out at ~50% confluency and cells were transfected with the indicated concentration of RAB oligonucleotides (see oligonucleotide chart and Figure Legends) using Lipofectamine RNAi/MAX (Invitrogen) for 48 h. All siRNA knock-down experiments were validated by immunoblotting.

4.3. Immunoblotting

Cells in culture were washed three times with pre-chilled PBS and harvested with a rubber cell scraper. Cell pellets were resuspended in lysis buffer containing 50 mM Tris-HCl pH 7.4, 150 mM NaCl, 1% NP-40, 0.5% sodium deoxycholate and freshly added protease inhibitor cocktail (Roche) for 1 h on ice. The cell lysates were then centrifuged at 1889 g at 4 °C for 10 min. The concentration of protein from each sample was measured with Bio-Rad protein assay (Bio-Rad, Hercules, CA), equalized, and boiled with 4X loading buffer. Proteins from either cell lysates or immunoprecipitations were separated by SDS-PAGE on 10% gels, and transferred onto nitrocellulose membranes (GE Healthcare, Chicago, IL). Membranes were blocked for 30 min at room temperature in PBS containing 0.3% (v/v) Tween-20 (PBST) and 5% dried milk, and then incubated overnight at 4 °C with diluted primary antibodies. Protein–antibody complexes were detected with HRP-conjugated goat anti-mouse-IgG (Jackson Research Laboratories, Bar Harbor, ME) or donkey anti-rabbit-IgG (GE Healthcare) secondary antibodies for 30 min at room temperature, followed by enhanced chemiluminescence substrate (ThermoFisher Scientific). Immunoblot images were acquired by iBright Imaging Systems (Invitrogen).

4.4. Immunofluorescence and microscopy imaging

Cells plated on coverslips were incubated with either 7 μg/ml Tf-568 or 1 μg/ml EGF-555 diluted in complete media for 15 min at 37 °C and then fixed in 4% paraformaldehyde

at room temperature for 10 min. After 3 rinses in PBS cells were incubated with primary antibodies to EEA1(Fig. 1) or RAB5 (Fig. 2) and appropriate fluorochrome–conjugated secondary antibodies diluted in staining buffer (PBS containing 0.5% bovine serum albumin and 0.2% saponin) for 30 min at room temperature. Cells were washed 3 times in PBS and mounted in Fluoromount G (SouthernBiotech). Z-stack confocal imaging was performed using a Zeiss LSM 800 confocal microscope (Carl Zeiss) with a Plan-Apochromat 63X/1.4 NA oil objective and appropriate filters and the images were assessed using Imaris software. Briefly, Z-sections of images (5 slices) were 3D-rendered with Imaris x64 9.1.2 software (Bitplane AG, Zurich, Switzerland). To obtain 3D-rendered surfaces, the smooth surface detail was set at 0.200 μm and the background subtraction at 0.543 μm. The area of the surfaces generated and the number of structures were quantified by Imaris (Oxford Instruments) and the values were exported into Excel for graphical and statistical analysis using GraphPad Prism 9 (GraphPad, San Diego, CA). For Supplemental Fig. 1, the Image J plug-in was used to obtain Manders' Overlap Coefficients from z-sections.

4.5. Statistical analysis

Data obtained from Imaris (Oxford Instruments) were exported to GraphPad Prism 9 (GraphPad, San Diego, CA). Bar graphs were created representing the mean and standard deviation from data obtained from three independent experiments. Normal distribution was assessed with the D'Agostino and Pearson normality test. Statistical significance was calculated with an unpaired two-tailed t-test for data that met a normal distribution, and with the Mann-Whitney non-parametric two-tailed test for non-normal distributions. No blinding was done in the experimentation.

Supplementary Material

Refer to Web version on PubMed Central for supplementary material.

Acknowledgments

The authors thank Tyler Jones for initial studies not included in the manuscript, and Ajay Murakonda for excellent technical assistance in analysis of the supplemental data.

Funding

This work was supported by the National Institutes of Health [grant number R35GM144102 from the National Institute of General Medical Sciences].

References

Ang AL, Folsch H, Koivisto UM, Pypaert M, Mellman I, 2003. The Rab8 GTPase selectively regulates AP-1B-dependent basolateral transport in polarized Madin-Darby canine kidney cells. J. Cell Biol 163, 339–350. [PubMed: 14581456]

de Araujo MEG, Liebscher G, Hess MW, Huber LA, 2020. Lysosomal size matters. Traffic 21, 60–75. [PubMed: 31808235]

Babbey CM, Ahktar N, Wang E, Chen CC, Grant BD, Dunn KW, 2006. Rab10 regulates membrane transport through early endosomes of polarized Madin-Darby canine kidney cells. Mol. Biol. Cell 17, 3156–3175. [PubMed: 16641372]

Babbey CM, Bacallao RL, Dunn KW, 2010. Rab10 associates with primary cilia and the exocyst complex in renal epithelial cells. Am. J. Physiol. Ren. Physiol 299, F495–F506.

Barbieri MA, Roberts RL, Mukhopadhyay A, Stahl PD, 1996. Rab5 regulates the dynamics of early endosome fusion. Biocell 20, 331–338. [PubMed: 9031602]

Benveniste M, Schlessinger J, Kam Z, 1989. Characterization of internalization and endosome formation of epidermal growth factor in transfected NIH-3T3 cells by computerized image-intensified three-dimensional fluorescence microscopy. J. Cell Biol 109, 2105–2115. [PubMed: 2808521]

Binda C, Genier S, Degrandmaison J, Picard S, Frechette L, Jean S, Marsault E, Parent JL, 2019. L-type prostaglandin D synthase regulates the trafficking of the PGD(2) DP1 receptor by interacting with the GTPase Rab4. J. Biol. Chem 294, 16865–16883. [PubMed: 31575663]

Brown FD, Rozelle AL, Yin HL, Balla T, Donaldson JG, 2001. Phosphatidylinositol 4,5-bisphosphate and Arf6-regulated membrane traffic. J. Cell Biol 154, 1007–1017. [PubMed: 11535619]

Bucci C, Parton RG, Mather IH, Stunnenberg H, Simons K, Hoflack B, Zerial M, 1992. The small GTPase rab5 functions as a regulatory factor in the early endocytic pathway. Cell 70, 715–728. [PubMed: 1516130]

Cai B, Xie S, Liu F, Simone LC, Caplan S, Qin X, Naslavsky N, 2014. Rapid degradation of the complement regulator, CD59, by a novel inhibitor. J. Biol. Chem 289, 12109–12125. [PubMed: 24616098]

Chen Y, Lippincott-Schwartz J, 2013. Rab10 delivers GLUT4 storage vesicles to the plasma membrane. Commun. Integr. Biol 6, e23779. [PubMed: 23713133]

Chen YT, Holcomb C, Moore HP, 1993. Expression and localization of two low molecular weight GTP-binding proteins, Rab8 and Rab10, by epitope tag. Proc. Natl. Acad. Sci 90, 6508–6512. [PubMed: 7688123]

Christoforidis S, McBride HM, Burgoyne RD, Zerial M, 1999a. The Rab5 effector EEA1 is a core component of endosome docking. Nature 397, 621–625. [PubMed: 10050856]

Christoforidis S, Miaczynska M, Ashman K, Wilm M, Zhao L, Yip SC, Waterfield MD, Backer JM, Zerial M, 1999b. Phosphatidylinositol-3-OH kinases are Rab5 effectors. Nat. Cell Biol 1, 249–252. [PubMed: 10559924]

Ciechanover A, Schwartz AL, Dautry-Varsat A, Lodish HF, 1983. Kinetics of internalization and recycling of transferrin and the transferrin receptor in a human hepatoma cell line. effect of lysosomotropic agents. J. Biol. Chem 258, 9681–9689. [PubMed: 6309781]

Conner SD, Schmid SL, 2003. Regulated portals of entry into the cell. Nature 422, 37–44. [PubMed: 12621426]

Corvera S, D'Arrigo A, Stenmark H, 1999. Phosphoinositides in membrane traffic. Curr. Opin. Cell Biol 11, 460–465. [PubMed: 10449332]

Daro E, van der Sluijs P, Galli T, Mellman I, 1996. Rab4 and cellubrevin define different early endosome populations on the pathway of transferrin receptor recycling. Proc. Natl. Acad. Sci 93, 9559–9564. [PubMed: 8790369]

Dilsizoglu Senol A, Tagliafierro L, Gorisse-Hussonnois L, Rebeillard F, Huguet L, Geny D, Contremoulins V, Corlier F, Potier MC, Chasseigneaux S, Darmon M, Allinquant B, 2019. Protein interacting with Amyloid Precursor protein tail-1 (PAT1) is involved in early endocytosis. Cell Mol. Life Sci 76, 4995–5009. [PubMed: 31139847]

Duclos S, Corsini R, Desjardins M, 2003. Remodeling of endosomes during lysosome biogenesis involves 'kiss and run' fusion events regulated by rab5. J. Cell Sci 116, 907–918. [PubMed: 12571288]

English AR, Voeltz GK, 2013. Rab10 GTPase regulates ER dynamics and morphology. Nat. Cell Biol 15, 169–178. [PubMed: 23263280]

Etoh K, Fukuda M, 2019. Rab10 regulates tubular endosome formation through KIF13A and KIF13B motors. J. Cell Sci 132.

Farmer T, Xie S, Naslavsky N, Stockli J, James DE, Caplan S, 2020. Defining the protein and lipid constituents of tubular recycling endosomes. J. Biol. Chem

Feng S, Knodler A, Ren J, Zhang J, Zhang X, Hong Y, Huang S, Peranen J, Guo W, 2012. A Rab8 guanine nucleotide exchange factor-effector interaction network regulates primary ciliogenesis. J. Biol. Chem 287, 15602–15609. [PubMed: 22433857]

Gorvel JP, Chavrier P, Zerial M, Gruenberg J, 1991. rab5 controls early endosome fusion in vitro. Cell 64, 915–925. [PubMed: 1900457]

Green EG, Ramm E, Riley NM, Spiro DJ, Goldenring JR, Wessling-Resnick M, 1997. Rab11 is associated with transferrin-containing recycling compartments in K562 cells. Biochem Biophys. Res Commun 239, 612–616. [PubMed: 9344879]

Haas AK, Fuchs E, Kopajtich R, Barr FA, 2005. A GTPase-activating protein controls Rab5 function in endocytic trafficking. Nat. Cell Biol 7, 887–893. [PubMed: 16086013]

Huber LA, Pimplikar S, Parton RG, Virta H, Zerial M, Simons K, 1993. Rab8, a small GTPase involved in vesicular traffic between the TGN and the basolateral plasma membrane. J. Cell Biol 123, 35–45. [PubMed: 8408203]

Jagath JR, De Maziere AM, Peden AA, Ervin KE, Advani RJ, Van Dijk SM, Klumperman J, Scheller RH, 2004. Rab14 is involved in membrane trafficking between the Golgi complex and endosomes. Mol. Biol. Cell

Jovic M, Sharma M, Rahajeng J, Caplan S, 2010. The early endosome: a busy sorting station for proteins at the crossroads. Histol. Histopathol 25, 99–112. [PubMed: 19924646]

Kageyama-Yahara N, Suehiro Y, Yamamoto T, Kadowaki M, 2011. Rab5a regulates surface expression of FcepsilonRI and functional activation in mast cells. Biol. Pharm. Bull 34, 760–763. [PubMed: 21532169]

Keil R, Hatzfeld M, 2014. The armadillo protein p0071 is involved in Rab11-dependent recycling. J. Cell Sci 127, 60–71. [PubMed: 24163434]

Knodler A, Feng S, Zhang J, Zhang X, Das A, Peranen J, Guo W, 2010. Coordination of Rab8 and Rab11 in primary ciliogenesis. Proc. Natl. Acad. Sci. USA 107, 6346–6351. [PubMed: 20308558]

Kobayashi H, Fukuda M, 2013. Arf6, Rab11 and transferrin receptor define distinct populations of recycling endosomes. Commun. Integr. Biol 6, e25036. [PubMed: 24255739]

Kobayashi H, Etoh K, Ohbayashi N, Fukuda M, 2014. Rab35 promotes the recruitment of Rab8, Rab13 and Rab36 to recycling endosomes through MICAL-L1 during neurite outgrowth. Biol. Open 3, 803–814. [PubMed: 25086062]

Kobayashi T, Gu F, Gruenberg J, 1998. Lipids, lipid domains and lipid-protein interactions in endocytic membrane traffic. Semin Cell Dev. Biol 9, 517–526. [PubMed: 9835639]

Kouranti I, Sachse M, Arouche N, Goud B, Echard A, 2006. Rab35 regulates an endocytic recycling pathway essential for the terminal steps of cytokinesis. Curr. Biol 16, 1719–1725. [PubMed: 16950109]

Linder MD, Uronen RL, Holtta-Vuori M, van der Sluijs P, Peranen J, Ikonen E, 2006. Rab8-dependent recycling promotes endosomal cholesterol removal in normal and Sphingolipidosis Cells. Mol. Biol. Cell

Linder MD, Uronen RL, Holtta-Vuori M, van der Sluijs P, Peranen J, Ikonen E, 2007. Rab8-dependent recycling promotes endosomal cholesterol removal in normal and sphingolipidosis cells. Mol. Biol. Cell 18, 47–56. [PubMed: 17050734]

Magadan JG, Barbieri MA, Mesa R, Stahl PD, Mayorga LS, 2006. Rab22a regulates the sorting of transferrin to recycling endosomes. Mol. Cell Biol 26, 2595–2614. [PubMed: 16537905]

Miaczynska M, Bar-Sagi D, 2010. Signaling endosomes: seeing is believing. Curr. Opin. Cell Biol 22, 535–540. [PubMed: 20538448]

Mu FT, Callaghan JM, Steele-Mortimer O, Stenmark H, Parton RG, Campbell PL, McCluskey J, Yeo JP, Tock EP, Toh BH, 1995. EEA1, an early endosomeassociated protein. EEA1 is a conserved alpha-helical peripheral membrane protein flanked by cysteine “fingers” and contains a calmodulin-binding IQ motif. J. Biol. Chem 270, 13503–13511. [PubMed: 7768953]

Murphy RF, Powers S, Cantor CR, 1984. Endosome pH measured in single cells by dual fluorescence flow cytometry: rapid acidification of insulin to pH 6. J. Cell Biol 98, 1757–1762. [PubMed: 6144684]

Naslavsky N, Caplan S, 2018. The enigmatic endosome - sorting the ins and outs of endocytic trafficking. J. Cell Sci 131.

Naslavsky N, Weigert R, Donaldson JG, 2003. Convergence of non-clathrin- and clathrin-derived endosomes involves Arf6 inactivation and changes in phosphoinositides. Mol. Biol. Cell 14, 417–431. [PubMed: 12589044]

Naslavsky N, Rahajeng J, Sharma M, Jovic M, Caplan S, 2006. Interactions between EHD proteins and Rab11-FIP2: a role for EHD3 in early endosomal transport. Mol. Biol. Cell 17, 163–177. [PubMed: 16251358]

Nossal R, Weiss GH, Nandi PK, Lippoldt RE, Edelhoch H, 1983. Sizes and mass distributions of clathrin-coated vesicles from bovine brain. Arch. Biochem Biophys 226, 593–603. [PubMed: 6139088]

Parton RG, Schrotz P, Bucci C, Gruenberg J, 1992. Plasticity of early endosomes. J. Cell Sci 103 (Pt 2), 335–348. [PubMed: 1478937]

Pearse BM, 1982. Coated vesicles from human placenta carry ferritin, transferrin, and immunoglobulin G. Proc. Natl. Acad. Sci. USA 79, 451–455. [PubMed: 6952195]

Pfeffer SR, 2017. Rab GTPases: master regulators that establish the secretory and endocytic pathways. Mol. Biol. Cell 28, 712–715. [PubMed: 28292916]

Rahajeng J, Giridharan SS, Cai B, Naslavsky N, Caplan S, 2012. MICAL-L1 is a tubular endosomal membrane hub that connects Rab35 and Arf6 with Rab8a. Traffic 13, 82–93. [PubMed: 21951725]

Ramanathan HN, Ye Y, 2012. The p97 ATPase associates with EEA1 to regulate the size of early endosomes. Cell Res 22, 346–359. [PubMed: 21556036]

Raposo G, Stoorvogel W, 2013. Extracellular vesicles: exosomes microvesicles, and friends. J. Cell Biol 200, 373–383. [PubMed: 23420871]

Robert A, Carpentier JL, Van Obberghen E, Canivet B, Gorden P, Orci L, 1985. The endosomal compartment of rat hepatocytes. its characterization in the course of [125I]insulin internalization. Exp. Cell Res 159, 113–126. [PubMed: 3896823]

Sato T, Mushiake S, Kato Y, Sato K, Sato M, Takeda N, Ozono K, Miki K, Kubo Y, Tsuji A, Harada R, Harada A, 2007. The Rab8 GTPase regulates apical protein localization in intestinal cells. Nature 448, 366–369. [PubMed: 17597763]

Schnatwinkel C, Christoforidis S, Lindsay MR, Uttenweiler-Joseph S, Wilm M, Parton RG, Zerial M, 2004. The Rab5 effector Rabankyrin-5 regulates and coordinates different endocytic mechanisms. PLoS Biol. 2, E261. [PubMed: 15328530]

Schuck S, Gerl MJ, Ang A, Manninen A, Keller P, Mellman I, Simons K, 2007. Rab10 is involved in basolateral transport in polarized Madin-Darby canine kidney cells. Traffic 8, 47–60. [PubMed: 17132146]

Sharma M, Giridharan SS, Rahajeng J, Naslavsky N, Caplan S, 2009. MICAL-L1 links EHD1 to tubular recycling endosomes and regulates receptor recycling. Mol. Biol. Cell 20, 5181–5194. [PubMed: 19864458]

Sharma M, Giridharan SS, Rahajeng J, Caplan S, Naslavsky N, 2010. MICAL-L1: an unusual Rab effector that links EHD1 to tubular recycling endosomes. Commun. Integr. Biol 3, 181–183. [PubMed: 20585517]

Simonsen A, Lippe R, Christoforidis S, Gaullier JM, Brech A, Callaghan J, Toh BH, Murphy C, Zerial M, Stenmark H, 1998. EEA1 links PI(3)K function to Rab5 regulation of endosome fusion. Nature 394, 494–498. [PubMed: 9697774]

Simpson JC, Griffiths G, Wessling-Resnick M, Fransen JA, Bennett H, Jones AT, 2004. A role for the small GTPase Rab21 in the early endocytic pathway. J. Cell Sci 117, 6297–6311. [PubMed: 15561770]

Sorkin A, Mazzotti M, Sorkina T, Scotto L, Beguinot L, 1996. Epidermal growth factor receptor interaction with clathrin adaptors is mediated by the Tyr974-containing internalization motif. J. Biol. Chem 271, 13377–13384. [PubMed: 8662849]

Terai T, Nishimura N, Kanda I, Yasui N, Sasaki T, 2006. JRAB/MICAL-L2 is a junctional Rab13-binding protein mediating the endocytic recycling of occludin. Mol. Biol. Cell 17, 2465–2475. [PubMed: 16525024]

Tubbesing K, Ward J, Abini-Agbomson R, Malhotra A, Rudkouskaya A, Warren J, Lamar J, Martino N, Adam AP, Barroso M, 2020. Complex Rab4-Mediated regulation of endosomal size and EGFR activation. Mol. Cancer Res 18, 757–773. [PubMed: 32019812]

Ullrich O, Reinsch S, Urbe S, Zerial M, Parton RG, 1996. Rab11 regulates recycling through the pericentriolar recycling endosome. J. Cell Biol 135, 913–924. [PubMed: 8922376]

van der Sluijs P, Hull M, Webster P, Male P, Goud B, Mellman I, 1992. The small GTP-binding protein rab4 controls an early sorting event on the endocytic pathway. Cell 70, 729–740. [PubMed: 1516131]

Van Der Sluijs P, Hull M, Zahraoui A, Tavitian A, Goud B, Mellman I, 1991. The small GTP-binding protein rab4 is associated with early endosomes. Proc. Natl. Acad. Sci. USA 88, 6313–6317. [PubMed: 1906178]

Vermeulen LMP, Brans T, Samal SK, Dubruel P, Demeester J, De Smedt SC, Remaut K, Braeckmans K, 2018. Endosomal size and membrane leakiness influence proton sponge-based rupture of endosomal vesicles. ACS Nano 12, 2332–2345. [PubMed: 29505236]

Villasenor R, Nonaka H, Del Conte-Zerial P, Kalaidzidis Y, Zerial M, 2015. Regulation of EGFR signal transduction by analogue-to-digital conversion in endosomes. Elife 4.

Vitale G, Rybin V, Christoforidis S, Thornqvist P, McCaffrey M, Stenmark H, Zerial M, 1998. Distinct Rab-binding domains mediate the interaction of Rabaptin-5 with GTP-bound Rab4 and Rab5. Embo J. 17, 1941–1951. [PubMed: 9524117]

de Wit H, Lichtenstein Y, Kelly RB, Geuze HJ, Klumperman J, van der Sluijs P, 2001. Rab4 regulates formation of synaptic-like microvesicles from early endosomes in PC12 cells. Mol. Biol. Cell 12, 3703–3715. [PubMed: 11694600]

Yang J, Yao W, Qian G, Wei Z, Wu G, Wang G, 2015. Rab5-mediated VE-cadherin internalization regulates the barrier function of the lung microvascular endothelium. Cell Mol. Life Sci 72, 4849–4866. [PubMed: 26112597]

Zeigerer A, Gilleron J, Bogorad RL, Marsico G, Nonaka H, Seifert S, Epstein-Barash H, Kuchimanchi S, Peng CG, Ruda VM, Del Conte-Zerial P, Hengstler JG, Kalaidzidis Y, Koteliansky V, Zerial M, 2012. Rab5 is necessary for the biogenesis of the endolysosomal system in vivo. Nature 485, 465–470. [PubMed: 22622570]

Zhang J, Reiling C, Reinecke JB, Prislan I, Marky LA, Sorgen PL, Naslavsky N, Caplan S, 2012. Rabankyrin-5 interacts with EHD1 and Vps26 to regulate endocytic trafficking and retromer function. Traffic 13, 745–757. [PubMed: 22284051]

Zuk PA, Elferink LA, 1999. Rab15 mediates an early endocytic event in Chinese hamster ovary cells. J. Biol. Chem 274, 22303–22312. [PubMed: 10428799]

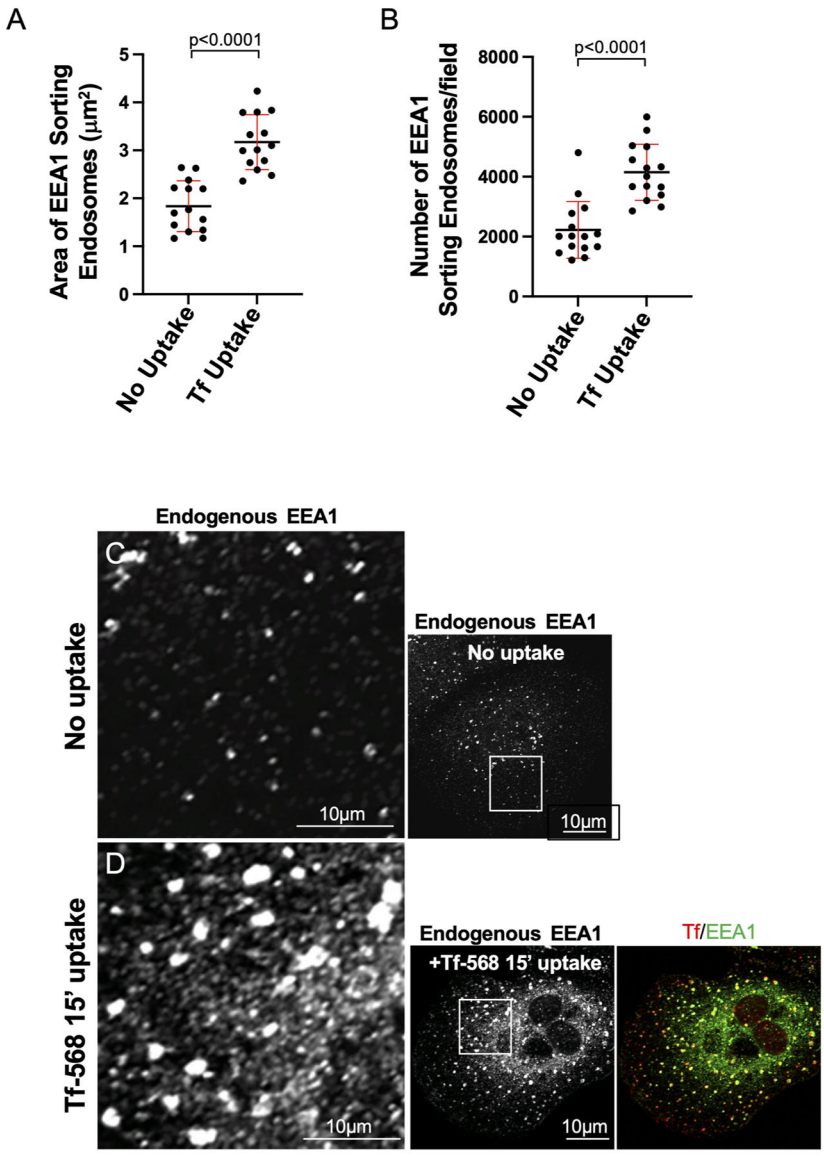

Fig. 1.

EE/SE size and number increase upon transferrin internalization. Non-small cell lung cancer cells were grown on cover-slips and either mock-treated or incubated with 1.4 ug/ml transferrin-568 (Tf-568) for 15 min. Cell were then fixed in 4% paraformaldehyde and subjected to immunostaining with antibodies to the EE/SE marker protein, EEA1. 4–5 images derived from 5 serial z-sections were obtained from 3 independent experiments and mean endosomal area of EEA1 structures (A) or number of EEA1-containing endosomes (B) were measured for cells incubated with or without Tf-568 using Imaris software. (C) Representative image and inset for cells with no Tf-568 uptake. (D) Representative image and inset for cells upon 15 min. Tf-568 uptake. The p-value for EE/SE size was calculated with an unpaired two-tailed t-test, because the data met the assumption for normality using the D'Agostino Pearson test. The p-value for EE/SE number was calculated with a Mann-

Whitney test, because the data did not meet the assumption of normality by the D'Agostino Pearson test.

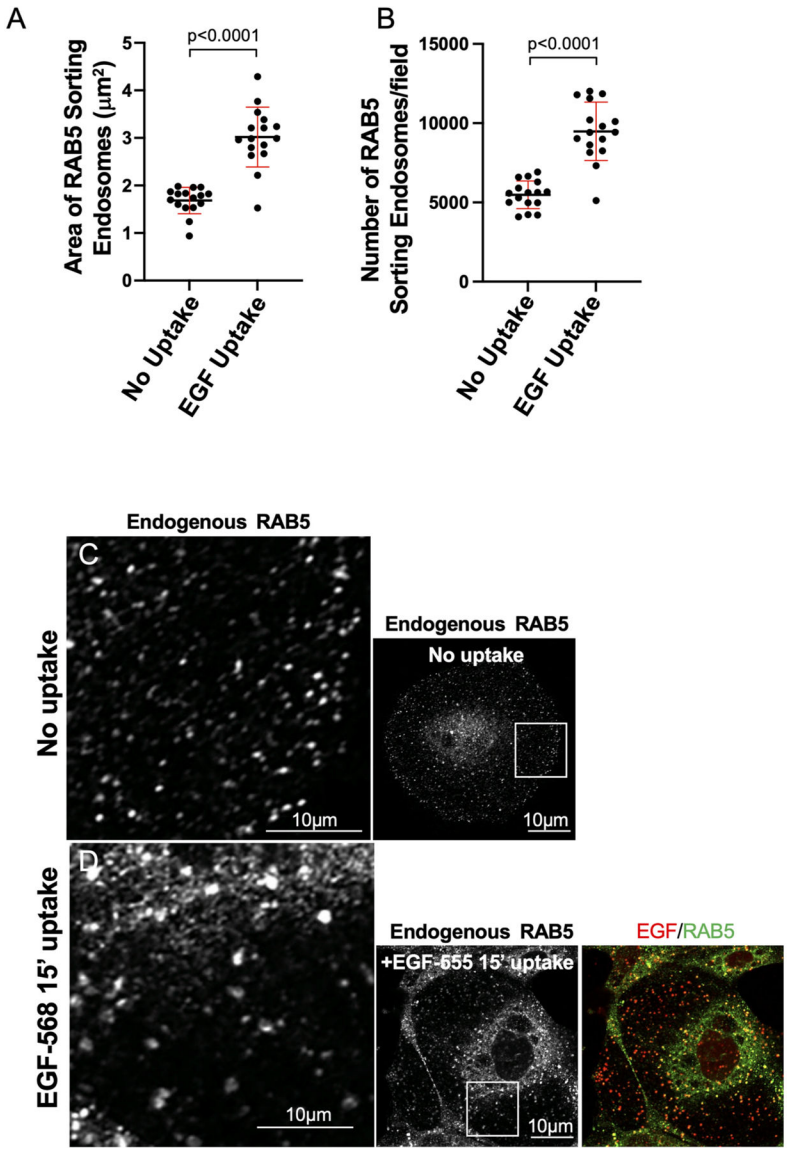

Fig. 2.

EE/SE size and number increase upon epidermal growth factor internalization. Non-small cell lung cancer cells were grown on cover-slips and either mock-treated or incubated with 2 ug/ml epidermal growth factor-555 (EGF-555) for 15 min. Cells were then fixed in 4% paraformaldehyde and subjected to immunostaining with antibodies to the EE/SE marker protein, RAB5. 4–5 images derived from 5 serial z-sections were obtained from 3 independent experiments and mean endosomal area of RAB5 structures (A) or number of RAB5-containing endosomes (B) were measured for cells incubated with or without EGF using Imaris software. (C) Representative image and inset for cells with no EGF uptake. (D) Representative image and inset for cells with EGF uptake. The p-value for EE/SE size was calculated with a Mann-Whitney test, because the data did not meet the assumption of normality by the D'Agostino Pearson test. The p-value for EE/SE number was calculated

with an unpaired two-tailed t-test, because the data met the assumption for normality using the D'Agostino Pearson test.

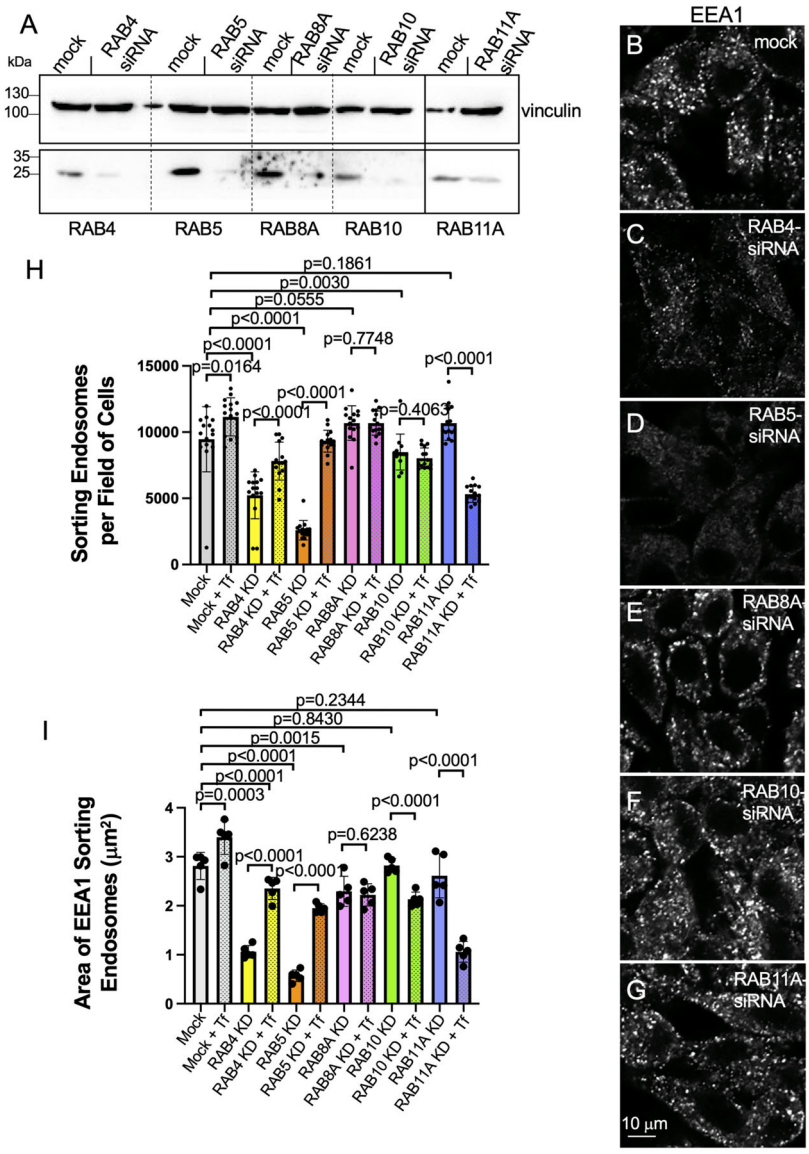

Fig. 3.

The number of EE/SE per cell is regulated by select endosomal RAB proteins. (A) HeLa cells were grown on cover-slips and 6-well plates and either mocktreated (transfection reagent only) or incubated with the following amounts of siRNA oligonucleotides specific for RAB4, RAB5, RAB8A, RAB10 or RAB11A per 2 ml well for 48 h: RAB4, 280 nmol; RAB5, 400 nmol; RAB8A, 600 nmol, RAB10, 400 nmol; RAB11A, 600 nmol. Cells from the 6-well plates were collected, lysed and subjected to immunoblot analysis with antibodies to RAB4, RAB5, RAB8A, RAB10 and RAB11 (to validate knock-down efficacy), and to vinculin (loading control). The solid line separating mock and RAB11A from the other RAB proteins indicates that this pair of lanes was run on a separate gel due to space constraints. Gels and images are representative of 3 independent experiments. (B-G) Representative images of cells immunostained for EEA1 upon mock-treatment (B), RAB4 siRNA-treatment (C), RAB5 siRNA-treatment (D), RAB8A siRNA-treatment (E), RAB10 siRNA-treatment

(F), RAB11A siRNA-treatment (G). (H) Graph illustrating the number of EE/SE observed per field of mock-treated and siRNA knock-down cells, with or without 15 min transferrin uptake. Data provided is a mean and standard deviation from 3 independent experiments. 3–5 images were obtained from each treatment, and Imaris software was used to measure EE/SE numbers. The p-values for EE/SE numbers were calculated with a Mann-Whitney test, because the data did not meet the assumption of normality by the D'Agostino Pearson or Kolmogorov-Smirnov tests. (I) Graph depicting the area of EEA1 endosomes observed per field of mock-treated and siRNA knock-down cells, with or without 15 min transferrin uptake. Data provided are mean and standard deviations from 3 independent experiments. 3–5 images were obtained from each treatment, and Imaris software was used to measure endosome area. The p-values for EEA1 endosome areas were calculated by t-test, as the data met the assumption of normality by the Kolmogorov-Smirnov test.